Pergamon

DEEP-SEA RESEARCH
PART II

Deep-Sea Research II 45 (1998) 617–642

Physical controls on dissolved inorganic radiocarbon variability in the California Current

Caroline A. Masiello[a,*], Ellen R.M. Druffel[a], James E. Bauer[b]

[a]*Department of Earth System Science, University of California at Irvine, Irvine, CA 92697-3100, USA*
[b]*School of Marine Science, College of William and Mary, P.O. Box 1346, Gloucester Point, VA 23062, USA*

Received 22 October 1996; in revised form 20 October 1997; accepted 20 October 1997

Abstract

We present depth profiles of $\Delta^{14}C$ and $\delta^{13}C$ of dissolved inorganic carbon (DIC) at Station M in the Eastern North Pacific. Several seasonal profiles are presented for the time period between 1991 and 1996. Comparison with GEOSECS data clearly shows changes in ocean radiocarbon profiles since 1973. The $\Delta^{14}C$ of DIC shows the most variability at depths of 450, 85, and 25 m, and the lowest variability at depths of 1600 and 2500 m. The largest variability in DIC $\Delta^{14}C$ occurs at 450 m, a depth marked by large fluctuations in the radiocarbon signatures of the source waters. The likely controls of DIC $\Delta^{14}C$ variability are physical changes in the circulation of the California Current System. A simple two-box model is used to show the importance of wind driven mixing at the surface. We discuss the likely effects of mesoscale eddies and ENSO on the DIC $\Delta^{14}C$ values at this site. We also show that remineralization of organic carbon (dissolved or particulate) is not responsible for the variability in the $\Delta^{14}C$ of DIC observed at Station M.

1. Introduction

The variability of seawater DIC $\Delta^{14}C$ is relevant to a number of oceanographic questions. First, the $\Delta^{14}C$ signature of DIC in seawater is a useful physical oceanographic tracer. Isotopic tracers provide a crucial piece of information lacking in stable tracers, and that is time. The half-life of ^{14}C is 5730 years, making it an ideal tracer for longer timescale physical oceanographic studies, such as the rate of circulation of the

* Corresponding author. Fax: 001 714 824 3256; e-mail; masiello@essgrad.ps.uci.edu.

0967-0645/98/$19.00
PII: S0967-0645(97)00096-9

ocean's conveyor (Broecker and Peng, 1982). Because of the input of bomb ^{14}C to the environment by nuclear weapons testing in the late 1950s and early 1960s, $\Delta^{14}C$ DIC data also have been used to address short timescale oceanographic questions, such as equatorial upwelling rates (Quay et al., 1983). Also, bomb ^{14}C is a useful tracer of the input rate of fossil fuel CO_2 to the environment.

The $\Delta^{14}C$ of DIC is relevant to studies of organic carbon cycling in the ocean as well. DIC is the inorganic precursor of all biological material produced in the ocean. In particular, DIC is the precursor of sinking organic material. This sinking material provides a rapid pathway between inorganic carbon at the ocean surface (a pool in equilibrium with atmospheric CO_2 and thus influenced by human perturbations) and carbon in ocean sediments (a pool stable on geologic time). Data on the radiocarbon variability of the parent DIC pool are necessary to interpret data on the radiocarbon variability of sinking organic material (see, e.g. (Druffel et al., 1996)).

Finally, the seasonal variability of the $\Delta^{14}C$ signature of DIC provides a constraint for paleoclimate studies. Major changes in ocean circulation patterns can be inferred from observed changes in proxies of DIC $\Delta^{14}C$, such as corals and foraminifera (see, e.g. (Broecker et al., 1984)). Identifying large changes in ocean circulation from DIC $\Delta^{14}C$ changes requires the ability to differentiate between short term climate fluctuations, such as seasonal, ENSO, and mesoscale variability, and variability caused by longer term climate changes processes, such as glacial–interglacial cycles. Estimates of short timescale variability have been made in the past using proxy records (Druffel, 1987; Druffel, 1989; Brown et al., 1993), and the variability of surface DIC $\Delta^{14}C$ has been modeled (Rodgers et al., 1997). Seasonal, open ocean variability in the $\Delta^{14}C$ of DIC has been measured in the Atlantic by Broecker and Peng (Broecker and Peng, 1980), who observed an approximate change of 35‰ between the fall and spring GEOSECS transits through similar areas. Changes in the $\Delta^{14}C$ of DIC have also been used to study coastal upwelling processes (Robinson, 1981). This paper presents direct observations of natural DIC $\Delta^{14}C$ variability as observed in seawater samples from a single ocean time-series station.

The variability reported here is likely the result of physical processes. The California Current has a seasonal cycle to its circulation patterns (Hickey, 1979; Lynn and Simpson, 1987) and has also been shown to be influenced by El Niño/Southern Oscillation (ENSO) (Hayward, 1993; Lynn et al., 1995). In addition to these large-scale sources of physical variability, Station M is located close to a semipermanent mesoscale eddy (Koblinsky et al., 1984). Variability in DIC $\Delta^{14}C$ at the surface can be connected to changes in wind-driven mixing, while mid-depth variability is more consistent with the effects of a mesoscale eddy.

The other possible causes of DIC $\Delta^{14}C$ variability are gas exchange between the atmosphere and surface ocean, and remineralization of organic carbon (fractionation during photosynthesis is not a possible cause of DIC $\Delta^{14}C$ changes because by definition $\Delta^{14}C$ values are $\delta^{13}C$-normalized). This paper shows that neither gas exchange nor remineralization of organic carbon could have caused measurable changes in the $\Delta^{14}C$ of DIC at this site during the 1990s.

2. Study site and cruises

Station M is located 220 km west of Point Conception, California (34°50′N, 123°00′W), and lies within the California Current System. The California Current System is composed of three currents: the southward-flowing California Current, the seasonal, northward-flowing Inshore Countercurrent (also called the Davidson Current), and the subsurface, northward-flowing California Undercurrent (Lynn and Simpson, 1987). The California Current is the dominant flow at Station M, and has been estimated to reach a maximum depth of 150 m in the spring and summer (Lynn and Simpson, 1987). Off Point Conception, the core of the California Current has been estimated to be 200–300 km west of the coast, placing Station M on the eastern edge of this equatorward flow. Station M is well west of the Inshore Countercurrent, and therefore does not see the seasonal reversal in flow direction associated with near-shore stations (Lynn and Simpson, 1987). At a depth of 250 m, the California Undercurrent extends only about 100 km offshore (Lynn and Simpson, 1987), but at a depth of 500 m, the flow can extend as far as 400 km offshore (Hickey, 1979). The California Current System is influenced by eddies, and the Point Conception region close to Station M is an area of enhanced eddy activity (see, for example, (Koblinsky et al., 1984; Sheres and Kenyon, 1990). At this site, the oxygen minimum occurs at approximately 700 m (Bauer et al., 1998).

We report data collected on 13 cruises to Station M: Pulse 7 (19–29 June 1991), Pulse 11 (19 February–2 March 1992), Pulse 12 (19 June–1 July 1992), Pulse 15 (15–27 October 1992), Pulse 16 (17–26 February 1993), Pulse 17 (14–23 July 1993), Pulse 18 (2–12 November 1993), Pulse 19 (3–12 February 1994), Pulse 20 (12–22 June 1994), Pulse 22 (13–26 September 1994), Pulse 25 (21 April–4 May 1995), Pulse 26 (1–14 June 1995), Pulse 29 (27 January–7 February 1996), and Pulse 30 (29 May–7 June 1996). Pulses 22 and 25 were on the *R/V Atlantis II*, Pulse 29 was on the *R/V Wecoma*; the others were on the *R/V New Horizon*. Nominal depths sampled were 25, 85, 450, 700, 1200, 1600, 2500 m, 600 m above bottom (approximately 3500 m), and 50 m above bottom (approximately 4050 m). A few cruises sampled additional nominal depths: on Pulse 17, a 5 m and a 150 m sample were collected, during Pulse 15 a 900 m sample was collected, and during Pulse 22, a 200 m sample was collected. The DIC data presented here are part of a long-term study of the carbon cycle at Station M (Bauer et al., 1996, 1988; Druffel et al., 1996, 1998).

3. Methods

Seawater was collected for $\Delta^{14}C$ DIC analysis in 12 or 30 l Go-Flo bottles deployed on a hydrowire. Reversing thermometers were placed on subsurface and deep bottles and, where available, corrected pressures are reported along with nominal depths in Table 1. In addition, a pinger was attached to the hydrowire below where the deepest two bottles (50 and 600 meters above bottom) were attached. This was done to ensure accurate positioning of the deepest bottles.

Table 1
$\Delta^{14}C$, $\delta^{13}C$, temperature, salinity, and σ_T data for Pulse cruises, June 1991–June 1996. Temperature data is from reversing thermometers except values in italics, which are from XBTs. The uncertainty for all variables is as stated in the text, except for the temperature data from Pulse 17, which are accurate to ± 0.1°C

CAMS#	UCID#	Date	Nominal depth (m)	Pressure (mb)	$\delta^{13}C$	$\Delta^{14}C$	*T*	salin.	sigma *T*
8522	WHA#279	Jul-91	30		1.1	49			
8521	WHA#278	Jul-91	450		−0.5	−125			
4904	WHA#346	Jul-91	700		−0.4	−186			
4903	WHA#345	Jul-91	1600	1644	−0.4	−240			
		Feb-92	25	20			13.63	32.83	24.62
		Feb-92	85	83			10.74	33.03	25.32
		Feb-92	450	449			5.84	34.16	26.94
4902	WHA#342	Feb-92	700	710	−0.3	−191	4.77	34.35	27.22
		Feb-92	1600	1649			2.57	34.56	27.6
4905	WHA#351	Feb-92	2500	2572	1.6	−238	1.75	34.65	27.73
		Feb-92	3500	3459			1.57	34.67	27.78
4906	WHA#352	Feb-92	4100	3832	0.0	−228	1.51	34.67	27.77
15232	453	Jun-92	25		2.4	70	*15.77*	32.99	24.29
15230	454	Jun-92	85		1.7	40	*11.17*	33.08	25.29
15229	455	Jun-92	450	456	−0.9	−144	6.00	34.05	26.83
		Jun-92	700	767			4.78	34.29	27.17
15231	458	Jun-92	1600	1629	−0.1	−242	2.48	34.57	27.63
17422	499	Jun-92	2500	2560	0.0	−242	1.74	34.46	27.58
15221	473	Jun-92	600 mab	3470	0.0	−248	1.57	34.66	27.77
17423	500	Jun-92	50 mab	4063	0.2	−237	1.50	34.68	27.78
19382	604	Oct-92	25	24	1.9	68	17.23	33.13	24.06
19383	605	Oct-92	85	73	1.1	76	11.49	33.20	25.31
17438	517	Oct-92	450	453	−0.3	−91	6.64	34.12	26.8
17436	515	Oct-92	700	716	−0.3	−166	5.01	34.29	27.13
17435	514	Oct-92	900	913	−0.3	−195	4.16	34.43	27.35
17434	513	Oct-92	1200	1225	−0.4	−230	3.34	34.51	27.49
17427	504	Oct-92	1600	1619	−0.2	−234	2.65	34.52	27.56
17426	503	Oct-92	2500	2530	−0.1	−247	1.79	34.63	27.72
17425	502	Oct-92	600 mab	3515	0.2	−233	1.56	34.67	27.77
17424	501	Oct-92	50 mab	4096	0.2	−221	1.50	34.64	27.75
17674	542	Feb-93	25		1.9	81	*13.75*	32.93	24.67
17675	543	Feb-93	450	471	−0.4	−123	5.37	34.13	26.97
17678	555	Feb-93	700	794	−0.5	−192	4.36	34.46	27.35
17676	553	Feb-93	1600	1606	−0.2	−251	2.57	34.57	27.61
17679	575	Feb-93	2500	2703	−0.1	−234	1.77	34.38	27.52
17677	554	Feb-93	3600	3766	−0.1	−216	1.56	34.67	27.78
17412	489	Jul-93	5		1.9	64			
17413	490	Jul-93	25		1.9	58			
17414	491	Jul-93	85		1.1	55			
17415	492	Jul-93	150		0.3	35			
17416	493	Jul-93	450		−0.3	−115			
17417	494	Jul-93	700	723	−0.4	−178	5.2		
17418	494	Jul-93	1600	1451	−0.3	−233	3.0		
17420	497	Jul-93	650 mab	3540	0.1	−239	1.5		
17421	498	Jul-93	50 mab	4239	0.1	−242	1.5		

Table 1 (Continued)

CAMS#	UCID#	Date	Nominal depth (m)	Pressure (mb)	$\delta^{13}C$	$\Delta^{14}C$	T	salin.	sigma T
19693	606	Nov-93	25		1.9	60		33.11	
24821	1319	Nov-93	85		0.4	23		33.44	
		Nov-93	450	450			5.74	34.17	26.95
		Nov-93	700	710			4.72	34.36	27.93
		Nov-93	1600	1589			2.67	34.60	27.62
		Nov-93	2500	2526			1.77	34.43	27.56
		Nov-93	50 mob	4084			1.51	34.13	27.34
23755	1038	Feb-94	25		1.2	69		33.10	
23756	1040	Feb-94	25		1.4	74			
23764	1219	Feb-94	85		1.8	76		33.10	
	1324	Feb-94	450	434	−0.5	−108	6.01	34.15	26.9
		Feb-94	700	662			4.98	34.35	27.2
		Feb-94	1600	2334			2.81	34.56	27.58
23762	1217	Feb-94	2500	2530	−0.2	−239	1.80	34.66	27.74
		Feb-94	650 mab	3547			1.58	34.47	27.6
23760	1127	Feb-94	50 mab	4096	−0.5	−220	1.52	34.55	27.68
21821	820	Jun-94	25		1.7	81		33.12	
21822	821	Jun-94	85		0.9	66		33.35	
21410	858	Jun-94	450	470	−0.3	−137	5.51	34.16	26.98
21411	859	Jun-94	700	720	−0.3	−176	4.71	34.35	27.22
21824	884	Jun-94	1600	1618	No data	−243	2.60	34.55	27.59
21823	883	Jun-94	2500	2460	0.0	−239	1.82	34.64	27.73
		Jun-94	600 mab	3459			1.56	34.68	27.78
		Jun-94	50 mab	4000			1.50	34.66	27.77
19699	612	Sep-94	25		2.0	65		33.28	
19697	610	Sep-94	85		0.3	68		33.44	
19703	617	Sep-94	200		0.2	2		33.98	
19698	611	Sep-94	450		−0.5	−125		34.16	
19695	608	Sep-94	700	687	−0.2	−166	4.84	34.38	27.23
19707	717	Sep-94	1200	1178	−0.4	−227	3.41	34.51	27.48
19696	609	Sep-94	1600	949	−0.1	−238		34.57	
19704	710	Sep-94	2500	2489	0.0	−250	1.80	34.65	27.74
19694	607	Sep-94	650 mab	3548	0.1	−237	1.56	34.68	27.78
19705	711	Sep-94	50 mab		No data	−224		34.69	
24816	1314	Apr-95	25		1.5	73			
	1317	Apr-95	85		0.8	52			
		Apr-95	700	656			4.88	34.28	27.15
		Apr-95	1600	1569			2.68	34.60	27.62
		Apr-95	650 mab	3505			1.49	34.67	27.78
		Apr-95	50 mab	4122			1.53	34.70	27.8
24817	1315	Jun-95	25		1.6	68	13.70	32.82	24.59
24822	1322	Jun-95	85		1.3	68	12.60	33.10	25.03
		Jun-95	200	256			7.49	33.99	26.59
	1610	Jun-95	450	475		−116	5.95	34.16	26.93
		Jun-95	700	722			4.94	34.33	27.18
		Jun-95	1200	1282			3.26	34.50	27.49
		Jun-95	1600					34.56	
		Jun-95	2500	2515			1.77	34.65	27.74

Table 1 (Continued)

CAMS#	UCID#	Date	Nominal depth (m)	Pressure (mb)	$\delta^{13}C$	$\Delta^{14}C$	T	salin.	sigma T
		Jun-95	650 mab	3466			1.52	34.68	27.78
		Jun-95	50 mab	4097			1.50	34.69	27.79
		Feb-96	25				14.10	33.58	25.1
		Feb-96	85				10.20	33.30	25.62
		Feb-96	200	205			7.99	33.99	26.51
	1820	Feb-96	450	451		−126	5.49	34.14	26.96
		Feb-96	700	685			4.51	34.32	27.21
		Feb-96	1200	1201			3.32	34.52	27.5
		Feb-96	1600	1597			2.65	34.58	27.6
		Feb-96	2500	2529			1.80	34.65	27.74
		Feb-96	600 mab	3555			1.54	34.68	27.78
		Feb-96	50 mab	4185			1.50		
		Jun-96	25					33.22	
		Jun-96	85					33.02	
		Jun-96	200	229			8.83	34.00	26.39
	1806	Jun-96	450	490		−79	5.49	33.96	26.82
		Jun-96	700	731			4.61	34.32	27.21
		Jun-96	900	971			4.04	34.58	27.48
		Jun-96	1600	1859			2.28	34.58	27.64
		Jun-96	2500	2742			1.73	34.66	27.75
		Jun-96	600 mab	3529			1.56	34.68	27.78
		Jun-96	50 mab	4078			1.51	34.68	27.78

After collection, seawater was filtered through precombusted (550°C) glass fiber filters (Gelman type A/E glass). One-half liter of seawater was poisoned with 100 µl saturated $HgCl_2$ solution, sealed, and stored at room temperature in precleaned glass reagent bottles. 250 ml of seawater were acidified and stripped of CO_2 using high purity N_2, which was recycled through the seawater (McNichol et al., 1994). This yielded approximately 6.5 mg of carbon as CO_2. The CO_2 was split into small aliquots (0.05 mg C) for $\delta^{13}C$ analysis and large (1 mg C) aliquots for subsequent conversion to graphite (Vogel, 1992). The $\Delta^{14}C$ of the graphite samples was determined at the Center for Accelerator Mass Spectrometry at Lawrence Livermore National Labs (LLNL). Seven of the samples (Pulses 7 and 11) were stripped of CO_2 at the National Ocean Sciences AMS Facility (NOSAMS) at the Woods Hole Oceanographic Institution and then converted to graphite and measured for $\Delta^{14}C$ at LLNL. $\Delta^{14}C$ values are reported as described by Stuiver and Polach (Stuiver and Polach, 1977) for geochemical samples without known age correction.

As part of this study, we measured both the mass and ^{14}C signature of the sample preparation blank. After stripping seawater that had been previously acidified (and therefore had no DIC), we concluded that approximately 0.02 to 0.04 mg of CO_2 were added during the stripping process. The amount of CO_2 added during graphitization was less than 0.01 mg. The amount of modern carbon added during stripping and graphitization was measured by processing seawater samples containing

approximately 6.5 mg of ^{14}C-free CO_2 (dissolved mineral calcite, initial $\Delta^{14}C = -1000‰$). After processing, the average $\Delta^{14}C$ of these samples was $-993 \pm 5‰$ ($n = 4$). Sources of blank constituted less than 0.8% of the sample, and total blank corrections ranged from $+0.4‰$ for surface samples to less than $+2.0‰$ for deep samples. Note that both of these values are well within the $\pm \sigma$ uncertainty of the AMS measurements (5.5‰).

To estimate the experimental uncertainty of the $\delta^{13}C$ and $\Delta^{14}C$ measurements (1σ error) 11 seawater samples of differing isotopic values were split in a CO_2-free glove box into separate bottles after collection and before CO_2 stripping. Both halves were measured for DIC $\delta^{13}C$ and $\Delta^{14}C$. One sample was split in thirds, yielding three DIC isotopic measurements. We used this data set to estimate the experimental uncertainty for all the samples reported here. We calculated the 1σ experimental uncertainty by taking the square root of the arithmetic mean of the squares of the standard deviations of data pairs, or $\sqrt{\Sigma(sd^2)/(n-1)}$. This yielded a $1\sigma = 4.5‰$ ($n = 12$) for the $\Delta^{14}C$ uncertainty and a $\delta^{13}C$ uncertainty of 0.2‰. Because a $\Delta^{14}C$ 1σ uncertainty of 4.5‰ is lower than the average counting σ reported by LLNL (5.5‰), we have chosen to use the higher of the two (LLNL 1σ uncertainty of 5.5‰). For consistency, we report the $\Delta^{14}C$ values for the first 250 ml aliquot taken from the sample jar.

In the following sections, we discuss the experimental uncertainty (as determined above) as well as the data variability at a particular depth. The data variability is expressed in this paper as two times the standard deviation (2 s.d.) of the DIC $\Delta^{14}C$ values of all the samples collected at a given depth. We use the terminology "2 s.d." to distinguish the true data variability from the experimental measurement uncertainty, σ. We also report the data range, the largest value at a given depth minus the smallest value at that depth.

4. Results

The DIC $\Delta^{14}C$ and $\delta^{13}C$ measurements for all cruises are listed in Table 1. Figure 1 shows the DIC $\Delta^{14}C$ data for seven cruises plotted versus depth. The highest $\Delta^{14}C$ values are found at the surface, averaging 68‰ ($n = 11$, 2 s.d. = 20‰, range = 32‰). The highest DIC $\Delta^{14}C$ values are found at the surface because of the ocean's contact with the atmosphere (gas exchange with the atmosphere is the only significant source of $^{14}CO_2$ to the ocean). The $\Delta^{14}C$ values decrease rapidly with depth to 450 m (average = $-116‰$, $n = 10$, 2 s.d. = 40‰, range = 53‰). Below 450 m, the DIC $\Delta^{14}C$ values decrease more slowly, reaching an average minimum of $-241‰$ at 2500 m ($n = 8$, 2 s.d. = 11‰, range = 16‰). This corresponds to an intermediate water reservoir age of 2280 ± 60 years (using the true ^{14}C half-life, 5730 years). Below 2500 m, the $\Delta^{14}C$ values rise slightly to an average of $-229‰$ at 4050 m ($n = 6$, 2 s.d. = 18‰). This corresponds to a deep water reservoir age of 2150 ± 100 yr. It is not surprising that the 2500 m water is "older" than the deepest water, since the 2500 m water is the southward, return flow of Pacific Deep Water and has been cut off from the atmosphere longer than Pacific Bottom Water at this site (Fiadero, 1982; Mantyla and Reid, 1983).

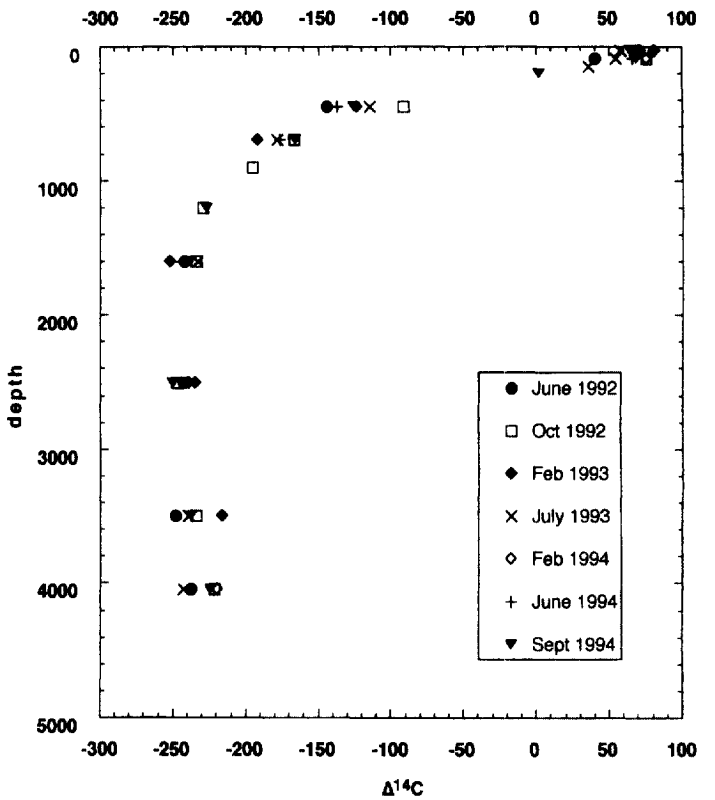

Fig. 1. DIC $\Delta^{14}C$ vs nominal depth for seven cruises to Station M from June 1992–June 1995.

Figure 2a shows the $\Delta^{14}C$ of DIC at 25 and 85 m plotted versus time. The lowest value measured at 25 m is 48‰ and the highest is 81‰, giving a range of 33‰ (6 times the 1 σ experimental error). The average DIC $\Delta^{14}C$ at 85 m is 57‰ ($n = 9$, 2 s.d. = 34‰), varying from 23‰ to 76‰, a range of 53‰ (almost 10 times the 1 σ experimental error). From 1994–1996 the DIC $\Delta^{14}C$ values at 25 and 85 m fluctuate out of phase from each other; high DIC $\Delta^{14}C$ values at 25 m correlate with low DIC $\Delta^{14}C$ values at 85 m, and vice versa.

Figure 2b shows 450, 700, and 1600 m DIC $\Delta^{14}C$ values vs. time. The 450 m data show the largest range of $\Delta^{14}C$ values, from -79‰ to -144‰, (a range of 65‰, or almost 12 times the 1 σ experimental error). The 450 m $\Delta^{14}C$ DIC values reached a minimum in June 1992 (-144‰), rose to a local maximum of -91‰ in October 1992, and then decreased to -123‰ in February 1993, close to the average for this depth. It is worth noting that reversing thermometers yielded a pressure difference of 3 mbar between the sample collection depths in June 1992 and October 1992. This corresponds to a depth difference of approximately 3 m, which is much too small to account for the variability observed here. The $\Delta^{14}C$ values at 450 m do not appear to

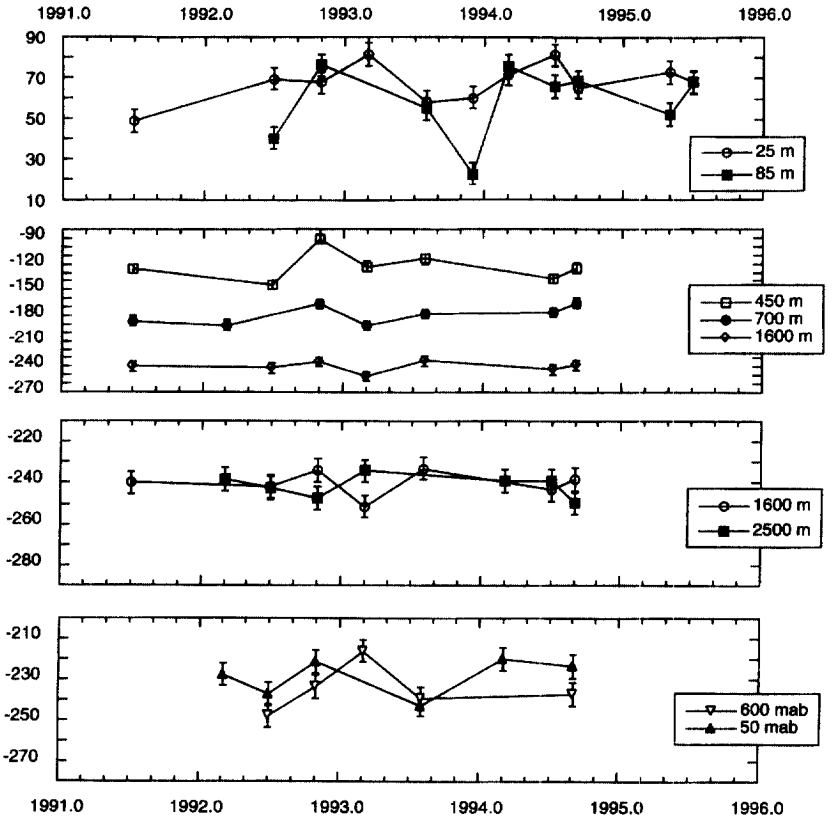

Fig. 2. (a) DIC $\Delta^{14}C$ at 25 and 85 m vs time, data from Table 1. (b) DIC $\Delta^{14}C$ at 450, 700 and 1600 m vs time, data from Table 1. (c) DIC $\Delta^{14}C$ at 1600 and 2500 m vs time, data from Table 1. (d) DIC $\Delta^{14}C$ at 600 mab and 50 mab vs time, data from Table 1.

vary with any relationship to the 25 m data, and there is not enough data to conclude whether or not the $\Delta^{14}C$ values at 450 m vary with any relationship to the 85 m $\Delta^{14}C$ values. However, the 450 m DIC $\Delta^{14}C$ data does appear to covary with the 700 and 1600 m data.

Figure 2c shows the $\Delta^{14}C$ DIC values plotted with time for 2500 m, where the lowest variability occurs. The 2500 m data variability is 11‰, exactly equal to our experimental uncertainty. Although the 1600 and 2500 m data sets appear to be inversely correlated, all changes at 2500 m are within our experimental uncertainty, and therefore no conclusions on this trend can be drawn.

Figure 2d shows DIC $\Delta^{14}C$ at 600 metres above bottom (nominal depth of 3500 m) and 50 metres above bottom (nominal depth of 4050 m). The range of $\Delta^{14}C$ values at 600 mab is 31‰ and at 50 mab is 23‰. These two sampling depths were often cast together, with a pinger placed on the hydrowire below the bottom bottle. Because of

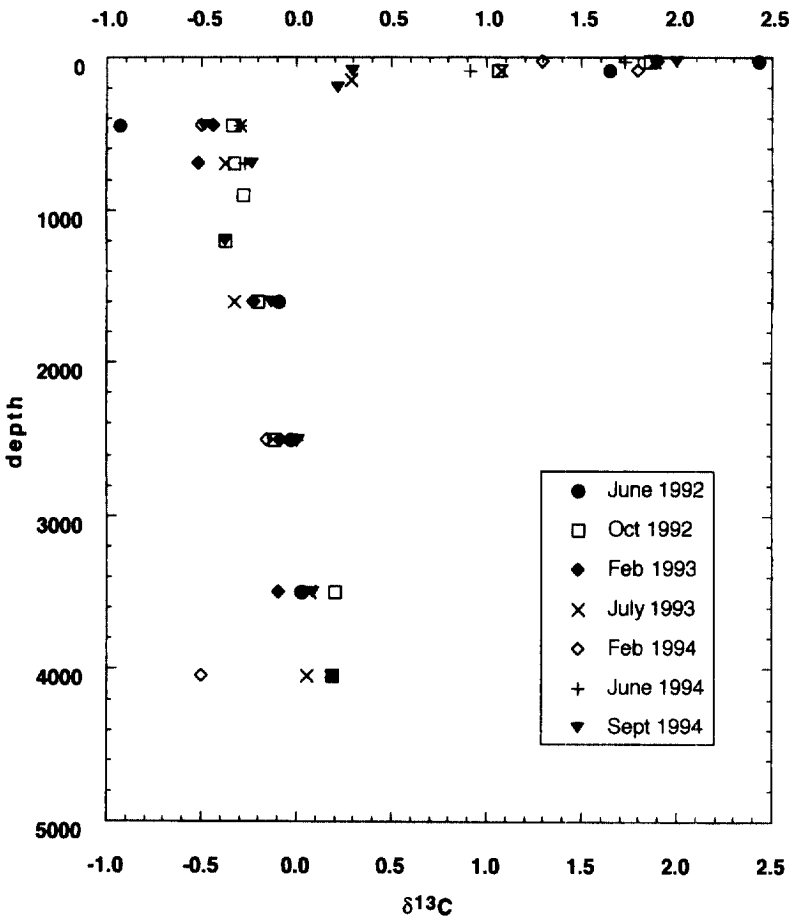

Fig. 3. DIC $\delta^{13}C$ vs nominal depth for 7 cruises to Station M from June 1992–June 1995.

this, the nominal depths of 50 mab and 600 mab are accurate to within $\pm$ 25 m from the bottom. The variation in bottom depth at this site is about 100 m, so bottles cast to 3500 and 4050 m are all within 125 m of their nominal depths.

Figure 3 shows $\delta^{13}C$ data plotted vs. depth for the same cruises as those in Fig. 1. $\delta^{13}C$ DIC values are highest in the surface, where plants preferentially photosynthesize $DI^{12}C$, leaving the remaining DIC enriched in ^{13}C. $\delta^{13}C$ values decrease with depth as remineralization adds ^{13}C depleted, photosynthetically fixed carbon back to the DIC pool (again, this has no effect on the DIC $\Delta^{14}C$ because $\Delta^{14}C$ is corrected for biological fractionation). The $\delta^{13}C$ of the upper 100 m shows substantial variability outside $\pm\sigma$ experimental error because of seasonal remineralization of biological material.

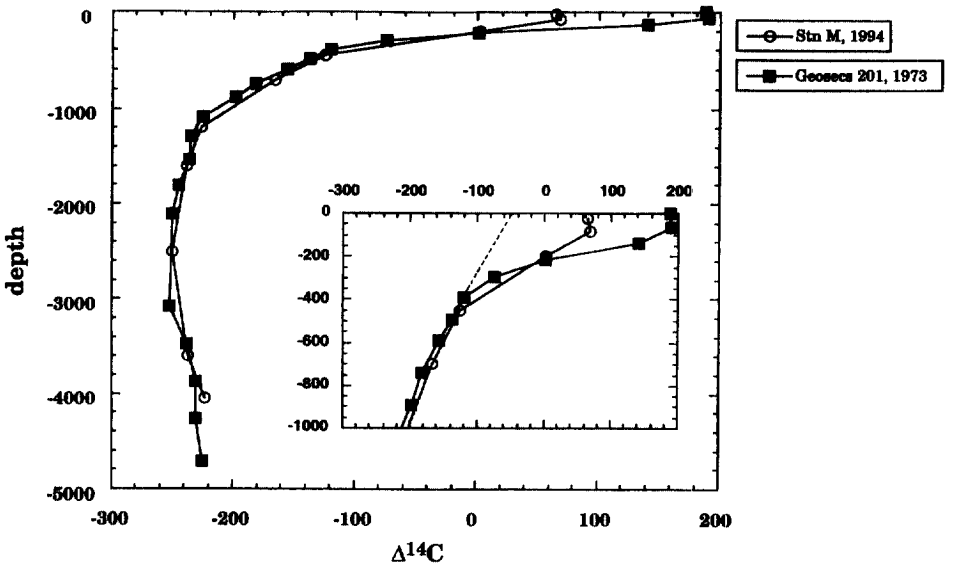

Fig. 4. DIC $\Delta^{14}C$ at Station M in September 1994 and at GEOSECS Station 201 in August 1973. The dotted line shows an estimate of the prebomb $\Delta^{14}C$ values at this site, based on modeling by Toggweiler et al. (Toggweiler et al., 1989) and on prebomb $\Delta^{14}C$ measurements (Druffel, 1987).

5. Discussion

5.1. Comparison with GEOSECS and WOCE Data

Figure 4 shows the most detailed profile available from Station M (September 1994) overlain with the profile from the closest GEOSECS site, station 201 (34°10′N, 127°53′W), occupied on 25 August 1973 (Ostlund and Stuiver, 1980). The profiles are virtually identical below 200 m. However, the upper 200 m of DIC $\Delta^{14}C$ values from the GEOSECS site are much higher, with the maximum differences at 25 and 85 m (see inset in Fig. 4). The 25 and 85 m GEOSECS DIC $\Delta^{14}C$ values in 1973 were + 189‰ and + 191‰, respectively, while the early 1990s average from 25 and 85 m at Station M were, respectively, + 68‰ ($n = 11$, 2 s.d. = 20‰) and + 57‰ ($n = 9$, 2 s.d. = 34‰). The DIC $\Delta^{14}C$ value of the surface ocean was much higher in 1973 because the bomb ^{14}C had less time to mix with deeper, ^{14}C-depleted waters and the terrestrial biosphere.

The similarity between intermediate depth DIC $\Delta^{14}C$ values in 1973 and the 1990s is likely the result of the years when samples were collected. Subtropical Pacific DIC $\Delta^{14}C$ values peaked around 1975 (Druffel, 1987), after the GEOSECS samples were collected and before the Station M samples were collected. Data taken in the North Central Pacific in 1985 (Druffel, 1989) show that in the mid-1980s, intermediate depth water was very high in comparison to either GEOSECS in 1973 or Station M in the

Table 2
Average Station M DIC $\Delta^{14}C$ data, range (largest value − smallest value at a given depth) and WOCE DIC $\Delta^{14}C$ data from 35.548°N, 122.863°W (Kay et al., 1996) and from 38°14′N, 124°15′W (Stuiver et al., 1996)

Stn M depth (m)	Station M average DIC $\Delta^{14}C$ (‰)	range of DIC $\Delta^{14}C$ (‰)	WOCE press. (dB)	WOCE DIC $\Delta^{14}C$ (‰)
25	68	33	39.6	68.6
85	57	53	65.6	49.2
450	−116	65	455.7	−125.4
700	−178	26	705.3	−180.0
1600	−240	18		
2500	−241	12	2576	−243.7
3500	−238	14	3507	−238.5
4050	−227	26		

1990s; North Central Pacific water at 482 m had a DIC $\Delta^{14}C$ value of +22‰. GEOSECS samples were likely collected as intermediate depths were seeing an increase in bomb ^{14}C, and the Stn. M samples were collected during the current slow decrease in bomb ^{14}C at intermediate depths. As models of the ocean distribution of bomb ^{14}C improve, interpretation of this data will become clearer. Below 450 m, the GEOSECS and Stn. M profiles are very similar. Note that both profiles show the oldest water occurring at intermediate depths (2500 m), indicative of the return flow of Pacific Deep Water (Mantyla and Reid, 1983).

The two WOCE stations closest to Station M are Station 5, cruise P17C, at 35.548°N, 122.863°W, sampled June 1991 (Key et al., 1996) and Station 10, cruise P17N, at 38°14′N, 124°58′W, sampled May 1993 (Stuiver et al., 1996). Station 5, cruise P17C was sampled from the surface to approximately 1100 m deep and small volume samples were measured by AMS, while Station 10, cruise P17N was sampled from approximately 1800 to 3400 m and large volume samples were measured by conventional, high precision techniques. Where WOCE sampling depths are close to Station M sampling depths, all WOCE data fall within the range of Station M data, and most WOCE data compares favorably to the Station M average. Most importantly, at depths where the Station M variability is small (700–3500 m), WOCE high-precision conventional data agree with the Station M average to within less than 3‰ (Table 2).

5.2. *Gas exchange and DIC $\Delta^{14}C$ variability*

At times in the past 50 years, the difference in $\Delta^{14}C$ between the CO_2 in the atmosphere and the DIC in the ocean has been sizeable. For a period of time after the 1960's nuclear weapons tests, the difference between these two pools was as large as 800‰ (Nydal et al., 1979). When the atmosphere and ocean differed substantially in CO_2 $\Delta^{14}C$ values, the atmosphere–ocean gradient in radiocarbon was capable of driving large, seasonal shifts in the ^{14}C of surface-ocean DIC. Broecker and Peng

(Broecker and Peng, 1980) showed that seasonal changes in DIC $\Delta^{14}C$ occurred at GEOSECS sites and that these changes were likely caused by the air–sea exchange of radiocarbon.

In the mid-1990s the atmospheric radiocarbon signature was approximately 125‰ (Levin et al., 1995). Broecker and Peng (Broecker and Peng, 1980) used a simple box model to calculate the effects of air–sea exchange on an area of surface ocean with a DIC concentration of 2 mM and a varying mixed layer, which seasonally thinned to 50 m and seasonally was cut off from deep mixing for 6 months. When we repeat this calculation for the Station M mixed layer, it predicts a seasonal change in DIC $\Delta^{14}C$ of 5‰. Our assumptions are a surface-ocean DIC $\Delta^{14}C$ value of 68‰, an atmospheric CO_2 $\Delta^{14}C$ value of 125‰ (Levin et al., 1995), an air–sea CO_2 exchange rate of 20 moles $CO_2/(m^2\ yr)$ (Broecker and Peng, 1980), and a 50 m mixed layer cut off from the atmosphere for 6 months. A shift of 5‰ is substantially less than the range of 33‰ we observed at 25 m, leading us to conclude that gas exchange was not a significant cause of DIC $\Delta^{14}C$ variability.

5.3. *Organic matter remineralization and DIC $\Delta^{14}C$ variability*

One potential cause of variability in the $\Delta^{14}C$ of DIC is seasonal change in the remineralization of organic matter. The source organic matter in the ocean can be classified into two pools: dissolved organic carbon (DOC), which is operationally defined as organic matter that passes through a 1 μm filter, and particulate organic carbon (POC), which is that organic matter retained on a 1 μm filter (Druffel et al., 1992). A portion of the falling POC (POC_{sink}) is broken down into smaller particles which remain suspended (POC_{susp}). Each of these forms of organic carbon can be converted to DIC via remineralization. This remineralization is an unlikely cause of changes in the $\Delta^{14}C$ of DIC because the DIC pool is much larger than either the POC or DOC pools. The concentration of DIC at Station M is approximately 2.0 mM, while the concentrations of DOC and POC are approximately 40–100 μM and 0.1–5 μM, respectively (Bauer et al., 1996; Druffel et al., 1996). We show below that none of these pools can put enough carbon into the DIC pool to affect the DIC $\Delta^{14}C$ signature.

In the following section, we consider three cases for the input of carbon from organic pools to the DIC pool: a transfer of carbon 1) from the POC_{susp} pool to the DIC pool, 2) from the DOC pool to the DIC pool, and 3) from the POC_{sink} pool to the DIC pool. We construct each case using the largest possible flux of carbon from the organic pools to the DIC pool, and we show that under these very high flux scenarios, each of these three cases does not measurably change the $\Delta^{14}C$ of DIC. From this, we conclude that organic matter remineralization is an unlikely explanation for DIC $\Delta^{14}C$ variability.

Case 1: Remineralization of POC_{susp} to DIC.

There are two scenarios for *in situ* POC_{susp} remineralization to DIC: (a) at the ocean surface, and (b) at depth. At the ocean surface, phytoplankton photosynthesize organic carbon from DIC and bacteria remineralize this organic carbon back to DIC. This cycle is rapid and occurs only in the mixed layer (< 100 m). Because the surface DIC is the carbon source for this POC, the $\Delta^{14}C$ values of the two pools are virtually

identical (Williams and Linick, 1975). This means that exchange of carbon between these two pools cannot be seen in the $\Delta^{14}C$ values. Thus, surface remineralization of POC is not a cause of DIC $\Delta^{14}C$ variability.

At depth, POC_{susp} remineralization adds carbon with a higher $\Delta^{14}C$ to an older, deep DIC pool. POC_{susp} remineralization would cause the largest change in the $\Delta^{14}C$ of DIC where the $\Delta^{14}C$ of these two pools are the most different and the flux between pools is the largest. The greatest difference in $\Delta^{14}C$ occurs at 2500 m, where the $\Delta^{14}C$ of DIC is approximately $-240‰$ and the $\Delta^{14}C$ of POC_{susp} is approximately $-10‰$ (Druffel et al., 1996). The concentration of POC_{susp} below the surface is between 0.1 and 1 μM (Druffel et al., 1996). We construct a scenario of maximum possible flux by assuming the largest concentration of POC_{susp}(1 μM) and the largest $\Delta^{14}C$ difference (230‰). Adding 1 μM carbon at $\Delta^{14}C = -10‰$ to 2 mM carbon at $\Delta^{14}C = -240‰$ causes a shift in the larger DIC pool of 0.1‰, considerably less than the variability reported here for DIC $\Delta^{14}C$ at 450 m and lower (a range of 65‰ at 450 m, see Fig. 2b). Remineralization of POC_{susp} below the surface layer is not a possible source of DIC $\Delta^{14}C$ variability.

Case 2: Remineralization of DOC to DIC.

At all depths, the $\Delta^{14}C$ of DOC is less than that of the DIC (Druffel et al., 1992) so exchange between these pools could potentially cause changes in the $\Delta^{14}C$ of DIC and DOC. The concentration of DOC at Station M has been shown to vary by 15 μM at the surface and approximately 5 μM below the surface over the period July 1991 to July 1993 (Bauer et al., 1998). An upper limit for the effects of DOC remineralization on the DIC pool is calculated by assuming that *all* of the DOC concentration variability results from remineralization of DOC to DIC, adding ^{14}C-depleted DOC carbon to the DIC pool. The maximum effect on the $\Delta^{14}C$ of DIC would occur at the depth where both the DOC concentration variability is the highest and the difference between the $\Delta^{14}C$ of the two pools is the largest. This occurs at the surface, where the DOC variability is 15 μM and the $\Delta^{14}C$ of the two pools is $+68‰$ (DIC) and $-240‰$ (DOC). 15 μM of DOC at $-240‰$ added to 2.00 mM DIC at $+68‰$ (the 25 m average DIC $\Delta^{14}C$) would cause a DIC $\Delta^{14}C$ shift of 2‰. This is within the uncertainty reported (1 σ experimental uncertainty of 11‰) and a factor of 10 less than the variability observed at 25 m (2 s.d. = 20‰).

Another scenario where the DOC pool could add old carbon to the DIC pool is one of rapid equilibrium, where organic processes rapidly transfer carbon back and forth between the DIC and DOC pools. However, this scenario is implausible given the radiocarbon age of the deep DOC pool (4000–6000 years; (Williams and Druffel, 1987)). The age disparity between DOC and DIC is too great to support rapid equilibrium between the two pools. This scenario becomes even more unlikely when we consider that for DOC remineralization to add enough ^{14}C-depleted carbon to significantly change the $\Delta^{14}C$ of DIC, it must be only the *old* portion of the DOC pool moving rapidly into the DIC pool.

Case 3: Remineralization of POC_{sink} at depth.

The third scenario where organic matter remineralization could influence the $\Delta^{14}C$ of DIC is the remineralization of POC_{sink} below 100 m. An upper bound for this flux can be calculated by assuming that all of the new production at Station M is

remineralized in a small volume at depth, adding its carbon to the DIC pool in that depth range. To do this calculation, we chose a volume of 200 m^3 at the depth between 350 and 550 m, with the $\Delta^{14}C$ equal to the average value at 450 m, or $-116‰$. An upper bound assumption for the primary productivity was made by taking the highest CalCOFI cruise mean for the California Current System from 1984–1994, 1300 mg $C/m^2/0.5$ d (Hayward et al., 1994), and assuming that this level of productivity occurred 24 h a day for 90 d and produced organic matter with a $\Delta^{14}C = 68‰$ (the average DIC $\Delta^{14}C$ at 25 m). With an f ratio = 0.1, the effect of remineralization of this material at depth is a shift in the deep $\Delta^{14}C$ of 1‰, a very small number compared to the range of data at 450 m (65‰).

A similar calculation can be done for the effect of the remineralization of POC_{sink} on the DIC $\Delta^{14}C$ at 3500 m (650 mab) and 4050 m (50 mab.) This calculation yields an even smaller shift than the calculation for 450 m, because the concentration of POC_{sink} is much lower at 3500 and 4050 m than at 450 m.

From these three cases, we conclude that exchange between organic and inorganic carbon pools is an unlikely cause of the DIC $\Delta^{14}C$ variability observed at Station M. It seems much more likely that the variability reported here was caused by physical processes.

5.4. *Physical controls on DIC $\Delta^{14}C$ variability*

Since DIC $\Delta^{14}C$ is not influenced by biological processes, then physical processes must be causing the changes we report here. There are a number of different physical processes that could cause significant fluctuations in the $\Delta^{14}C$ of DIC. At the surface, there is seasonal and ENSO-related variability in the California Current System. The surface and intermediate depths are likely influenced by the mesoscale eddy located just to the west of Station M. Variability at the deepest levels is likely the result of larger-scale physical events, such as Rossby or gravity waves in the deep ocean.

Mixed layer DIC $\Delta^{14}C$ variability. The variability of DIC $\Delta^{14}C$ observed at 25 and 85 m is significantly larger than experimental error (see Fig. 2a). In addition, the 25 and 85 m DIC $\Delta^{14}C$ values are inversely correlated; i.e. when the DIC $\Delta^{14}C$ is high at 25 m, it is low at 85 m, and vice versa. There are a number of physical processes that we would expect to cause surface DIC $\Delta^{14}C$ to vary. Among these are the seasonal thickening of the thermocline due to wind mixing, the quasiseasonal appearance of the Point Conception Eddy, and ENSO-related changes in the California Current System.

The average wind speed at Station M is 7.6 m/s (COADS monthly climatology, 1946–1989; (Woodruff and Lubker, 1993)), and this site has two maxima per year in wind speed. The average wind speed rises in March to 8.0 m/s, reaches a maximum in May of 8.6 m/s, decreases to the lowest monthly average of 6.8 m/s in September, and then rises again to a lower peak of 7.2 m/s in November (see Fig. 5). Higher wind speeds deepen the mixed layer, which should result in lower DIC $\Delta^{14}C$ values at 25 m and higher DIC $\Delta^{14}C$ values at 85 m. XBT data do show cruise to cruise variations in mixed layer depth, ranging from 40 to 100 m; however, the variations do not clearly match annual average windspeed data or DIC $\Delta^{14}C$ data. The connection between

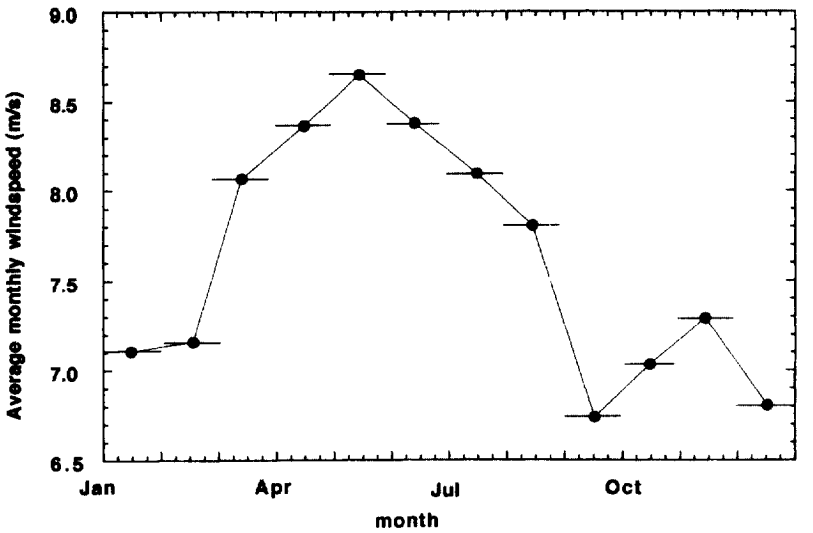

Fig. 5. Climatological average windspeed between 1946 and 1989 at 35°N, 123°W, taken from the COADS databased (Woodruff, 1993) (#42).

windspeed; mixed layer depth, and DIC $\Delta^{14}C$ values becomes clearer when modeled using month to month windspeed data instead of annual averages.

6. Model results

To understand whether or not wind mixing was the dominant control on DIC $\Delta^{14}C$ at this site, we constructed a simple, two-box model of the DIC $\Delta^{14}C$ in the mixed layer and thermocline at Station M. This model calculates the effect of wind-driven deepening of the mixed layer on DIC $\Delta^{14}C$ by making repeated mass balance calculations. The model was forced by only wind-driven mixing, with the goal of determining whether or not wind mixing was the major control on the DIC $\Delta^{14}C$ at 25 and 85 m. The other major assumption of this model is that the water in the upper 90 m at Station M is flushed monthly. Changes resulting from atmospheric input of bomb ^{14}C were neglected, as recent three-dimensional model calculations have shown that the bomb radiocarbon inventory in the ocean was essentially constant in the early 1990s (Duffy and Caldeira, 1995). The initial $\Delta^{14}C$ for the surface box was set at 85‰ (FM = 1.085), an upper bound for surface DIC $\Delta^{14}C$ values, and the initial $\Delta^{14}C$ of the deep box was set at 35‰ (FM = 1.035), a lower bound for 85 m DIC $\Delta^{14}C$ values.

A schematic of the model is shown in Fig. 6. The equations used are as below:

$$\text{Box A: } FM_A = (Z_A/ML)*(FM_A) + [(ML - Z_A)/ML]*(FM_B) \quad (1)$$

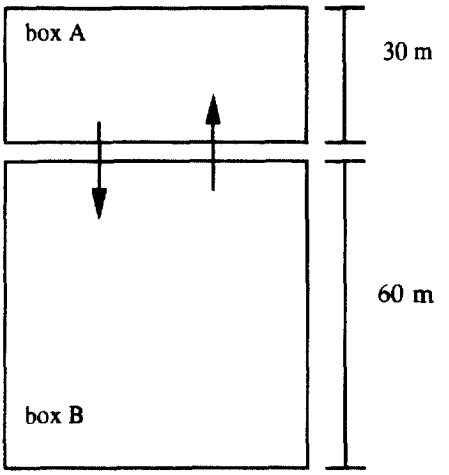

Fig. 6. Schematic of model used.

$$\text{Box B: } FM_B = [[(Z_B - (ML - Z_A)]/Z_B] * (1.035) + [(ML - Z_A)/Z_B] * (FM_A) \quad (2)$$

where $Z_A = 30$, the height of box A in meters, and $Z_B = 60$, the height of box B in meters. In this model, the depth of the mixed layer (ML) is a function of the wind speed only, and is calculated as below:

$$ML = ML_{max}(\text{windspeed} - 2.5)/(\text{windspeed}_{max} - 2.5). \quad (3)$$

Windspeed_{max} is 12 m/s, an upper bound of the COADS data at 35°N, 123°W from 1990 to 1993. Windspeed data is only available through December 1993, so model comparisons are only possible during this period. ML_{max} is 100 m, based on numerous XBT deployments on several cruises to Station M (Druffel and Bauer, unpublished data). The equation for ML is normalized to give ML = 30 m when wind speed is 5.5 m/s, the minimum windspeed reported in the COADS dataset for the Station M area.

Figures 7a and b show the model results overlain with 25 and 85 m DIC $\Delta^{14}C$ data. At 25 m the model matches all data points within experimental error bars, with the exception of one: Pulse 7, June 1991. This period was the highest POC_{sink} flux ever measured at Station M (K. Smith, personal communication) and may have experienced unusual circulation conditions. The match between all of the other DIC $\Delta^{14}C$ data points and the wind-driven model suggests that wind-speed changes are related to the variability in DIC $\Delta^{14}C$ values in the upper 25 m. Wind-speed changes may directly control the DIC $\Delta^{14}C$ values by deepening the thermocline and bringing up ^{14}C-depleted intermediate waters. It is also possible that changes in the windspeed are indirectly related to the DIC $\Delta^{14}C$, as increased wind-speed correlates with increased

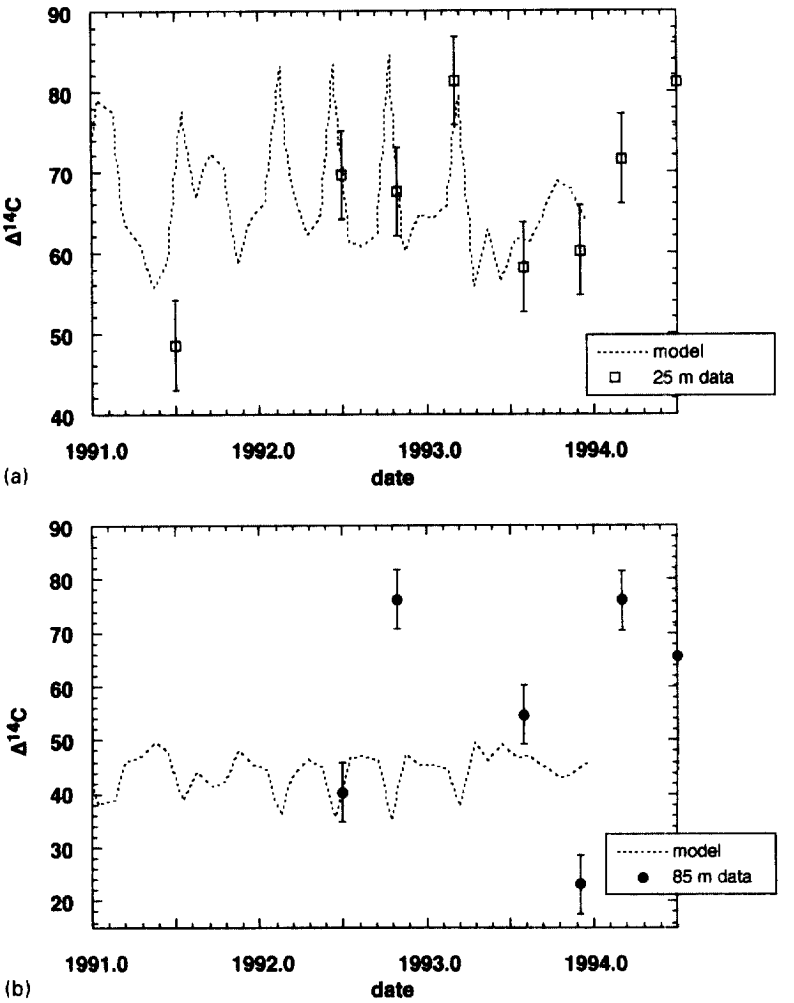

Fig. 7. Model results and DIC $\Delta^{14}C$ data at (a) 25 m and (b) 85 m.

flow of the California Current. The model results also clearly show that we have not sampled the Station M water column frequently enough to represent adequately the changes in DIC $\Delta^{14}C$ that occur.

As shown in Fig. 7b, at 85 m the model results do not match the data. Not only are the data points out of range of the model, the model does not even show the appropriate amplitude. Varying the size of the deep box does not improve the fit; nor does varying the initial $\Delta^{14}C$ of the deep and surface boxes. Wind-driven mixing is not sufficient to explain the variability that we observe at 85 m. The magnitude of the changes observed here suggests that the source water at 85 m varies quasi-seasonally,

with higher $\Delta^{14}C$ water arriving during periods of high windspeed. This is consistent with the seasonal deepening of the California Current (Lynn and Simpson, 1987). The core of the California Current can be as shallow as 30 m and as deep as 150 m (Lynn and Simpson, 1987). Bottles cast to 85 m may have been sampling in and out of the California Current. Sampling in and out of the California Current could cause $\Delta^{14}C$ fluctuations of the amplitude observed here.

6.1. Intermediate depth DIC $\Delta^{14}C$ variability

There are a number of physical factors that might be expected to influence the $\Delta^{14}C$ of DIC at intermediate depths. Among these are mesoscale eddies and the El Niño–La Niña climate cycle.

A semipermanent eddy was first observed off Point Conception by Sverdrup and Fleming (1941). Owen (1980) noted the presence of an eddy off Point Conception in January and June of 1964. Koblinsky et al. (1984) cited ship and satellite data from 1950 onwards to state that a mesoscale feature centered at approximately 32°N, 124°W has been present consistently during observations of this region. Eddies in the California Current have been shown to be formed close to the coast and then move westward, carrying coastal waters out to sea (Jones et al., 1991). Sheres and Kenyon (1990) tracked a cyclonic eddy 100 km west of Pt. Arguello, northwest of Pt. Conception in March and April of 1983. Using AVHRR data, Sheres and Kenyon (1990) observed the entrainment of a cold jet of coastal water by the offshore eddy. The eddy Koblinsky et al. (1984) reported was approximately 200 km in diameter, reached a depth of at least 1450 m, and traveled south at 1 cm/s for approximately 100 d. Based on available data, it seems reasonable to conclude that Station M is in the vicinity of the semipermanent eddy off Point Conception, and that this eddy can reach depths greater than 1000 m.

The expected effects of an eddy on the $\Delta^{14}C$ of the DIC in intermediate depth water depends on the structure and history of the eddy. A cold-core eddy could affect DIC $\Delta^{14}C$ values by bringing deeper waters up, and a warm-core eddy would presumably have the opposite effect. If an eddy entrains coastal water (as described by Koblinsky et al. (1984)), it could leave the Station M area with a coastal DIC $\Delta^{14}C$ signal. The cold filaments reported to be associated with eddies (Jones et al., 1991) would have a similar effect.

The El Niño–La Niña climate cycle is another process that could potentially influence the $\Delta^{14}C$ of DIC in the upper ocean. ENSO has been shown to influence the California Current System in a number of ways. The 1991–1993 ENSO raised sea level, deepened the nutricline, and suppressed upwelling. Observations of the California Current System in February of 1992 showed that the northward-flowing countercurrent and undercurrent were anomalously broad and strong (Lynn et al., 1995). During the 1991–1993 ENSO, physical markers in the California Current System returned to near normal conditions during the spring and summer of 1992, but returned to ENSO conditions in the winter of 1992 (Lynn et al., 1995). Suppression of upwelling limits exchange between surface and intermediate water, raising the surface DIC $\Delta^{14}C$ and presumably lowering the DIC $\Delta^{14}C$ below the mixed layer.

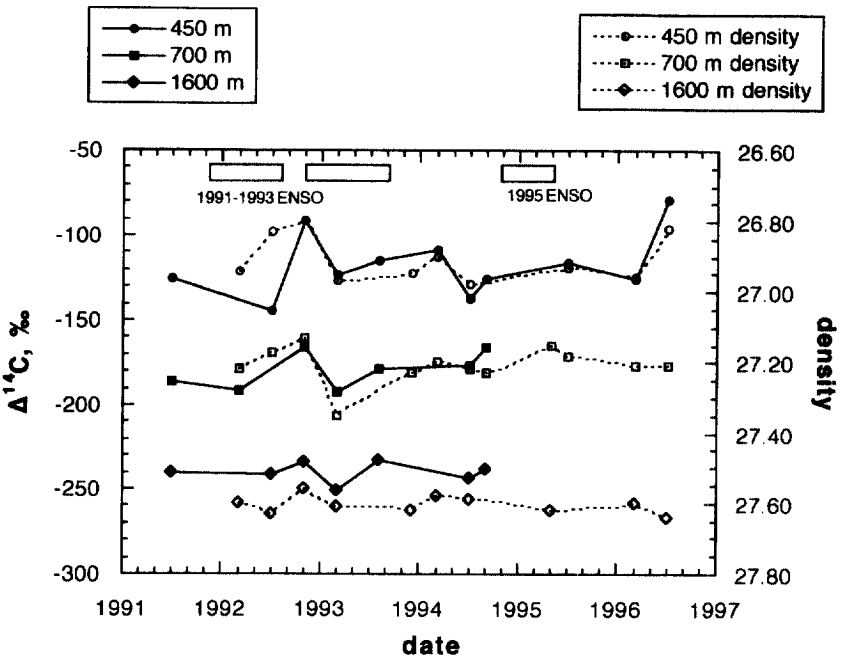

Fig. 8. DIC $\Delta^{14}C$ and density vs time at 450, 700 and 1600 m.

If the $\Delta^{14}C$ of DIC is indeed a sensitive tracer of physical oceanographic changes, then depths that show high variability in physical properties also should show high variability in DIC $\Delta^{14}C$. One commonly used physical tracer is density. A relationship between density and the $\Delta^{14}C$ of DIC is most likely to appear at intermediate depths, which are shallow enough to experience short-term mixing processes, but deep enough to remain unaffected by rainfall and sunlight, which could change salinity and temperature without necessarily affecting the $\Delta^{14}C$ of DIC. Additionally, the ^{14}C introduced into the environment by nuclear weapons testing is just now reaching intermediate waters in the Pacific. It is possible that bomb-contaminated and uncontaminated water masses are mixing at these depths, making the top of this depth range ideal for detecting a DIC $\Delta^{14}C$ mixing signal.

As expected, the correlation between physical tracers and radiocarbon appears clearest in the samples taken at 450, 700, and 1600 m. Figure 2b shows the $\Delta^{14}C$ of DIC between the depths of 450 and 1600 m, and Fig. 8 is an enlargement of Fig. 2b with σ_t (density) overlain, expanded to include data from 1996. Figure 8 shows an obvious correlation between density and DIC $\Delta^{14}C$, with the clearest correlation at 450 m, the depth of maximum DIC $\Delta^{14}C$ variability. Density and DIC $\Delta^{14}C$ covary for every data pair available except for one in June 1992. This sample was one of the first three processed in our lab, and as such may have a larger error associated with it. Without this point, a least-squares fit to the density and DIC $\Delta^{14}C$ data at 450 m

yields an r^2 of 0.90, a correlation significant to the 99% level. This graph unmistakably shows the physical nature of the mid-depth DIC $\Delta^{14}C$ changes: not only do changes in DIC parallel changes in density, but less dense waters are enriched in ^{14}C, as would be expected if more modern surface waters are mixing downward quasi-seasonally.

The other notable trend in Fig. 8 is that the DIC $\Delta^{14}C$ and density values at 450, 700, and 1600 m co-vary. In particular, an event occurred in mid-1992 that caused density and DIC $\Delta^{14}C$ to fluctuate rapidly at all three depths at the same time. The magnitude of this fluctuation is greatest at 450 m and least at 1600 m. This is consistent with the effects of an eddy. Lynn and Simpson (1990) showed that in 1985 the anticyclonic eddy located to the southwest of Station M caused a depression in the density field which affected depths at down to at least 1000 m. The density field depression was accompanied by a warm temperature anomaly, again affecting depths at least down to 1000 m. If anticyclonic eddies transport down warm surface water, they likely also transport down the higher DIC $\Delta^{14}C$ signature of these surface layers. It may be that during the 1992 ENSO, the eddy usually located just to the west of Station M moved to the east, causing the fluctuations in DIC $\Delta^{14}C$ that we report here.

6.2. *Stability at 2500 m*

The 2500 m depth showed the lowest DIC $\Delta^{14}C$ variability of all the depths sampled (Fig. 2c). 2 s.d. at 2500 m is 11‰, equal to the experimental uncertainty. An intercomparison with WOCE data from this depth is relevant: the Station M average value at 2500 m is -241‰, and the WOCE value at 2576 dB is -243.7‰ (Stuiver et al., 1996). These numbers are the same within the 3‰ error of the high precision WOCE measurements. DIC $\Delta^{14}C$ data suggest that this depth is the most stable at this site in the Pacific. This interpretation is consistent with the model of deep Pacific circulation put forth by Fiadero (1982), who suggested a mid-depth where vertical motion vanishes.

6.3. *Bottom water DIC $\Delta^{14}C$ variability*

DIC $\Delta^{14}C$ at 600 mab varies from -216‰ to -248‰, a range of 32‰, and at 50 mab DIC $\Delta^{14}C$ varies from -220‰ to -243‰, a range of 23‰ (Fig. 2d). Both of these ranges are considerably larger than the measurement error. The changes observed at 600 mab are particularly interesting, as this depth shows the fourth highest variability of all depths sampled. Few studies have been done on seasonal of interannual changes in the deep ocean, so little is known about potential causes. We identify two potential causes of the changes we observe at 600 mab.

The first possibility is that we sampled in and out of two water masses. In this area of the Pacific, the deepest water mass is the poleward flowing Pacific Bottom Water, which is overlain by the equatorward flow of North Pacific Deep Water (Mantyla and Reid, 1983). Even though North Pacific Deep Water (NPDW) lies on top of Pacific Bottom Water (PBW), NPDW is older than PBW (Ostlund and Stuiver, 1980). Thus

in the 1600–4100 m depth range, deeper casts produce younger water. However, silicate data from the closest GEOSECS site (201) show that the NPDW-PBW boundary occurs at a depth of about 2800 m. This is much higher than even the shallowest "600 mab" bottle, raising doubts that the DIC $\Delta^{14}C$ values vary because the 600 mab bottle was sampling in and out of two water masses.

The second possibility is that we observed real fluctuations in the PBW DIC $\Delta^{14}C$. These changes were not caused by the remineralization of organic matter. The amount of organic matter added to the deep ocean DIC pool is two orders of magnitude too small to perturb the DIC $\Delta^{14}C$ signature. The question remains what physical process could be the cause of these observed changes in the deep ocean.

Ample evidence exists to document the presence of current fluctuations in the deep Pacific. For example, Freeland (1993) monitored a site 1000 km to the west of Vancouver Island and found that while on the average, deep currents were sluggish, at times curents at 3000 m reached speeds of greater than 10 cm/s, which he hypothesized was caused by eddies. For comparison, typically the California Current travels at less than 25 cm/s (Lynn and Simpson, 1987). A high speed current would likely vary the physical properties of a water mass at a single site, including the water mass's DIC $\Delta^{14}C$ signature. At the Hawaii Ocean Timeseries site such variation in physical properties was observed in a 6 yr timeseries of temperature data from below 3500 m (Lukas and Santiago-Mandujano, 1996). The variations at the HOT site were periodic enough that the authors hypothesized a connection with baroclinic Rossby waves.

Beaulieu and Baldwin (1998) report deep flow oscillations at Station M from data collected during the mid-1990s. None of the current meter data show as dramatic changes as reported by Freeland (1993), but variability is clearly present on the timescale of 50–175 d. Although the Station M DIC $\Delta^{14}C$ deep values are undersampled relative to this time frame, our results are certainly consistent with 50–175 d oscillations in flow. Beaulieu and Baldwin (1998) also note that their results suggest the periodic advection of water from other locations. The periodic transport of water from other sites to Station M would likely cause fluctuations in the DIC $\Delta^{14}C$ signature. Unfortunately, the Station M current meter data set does not overlap in time with enough of the DIC $\Delta^{14}C$ data to allow comparison of the fluctuations in the two datasets. We can conclude only that our DIC $\Delta^{14}C$ data are consistent with the hypothesis that water masses from other locations are periodically transported to the seafloor at Station M.

7. Conclusions

The DIC $\Delta^{14}C$ data reported here show robust variability outside of the 2σ experimental error of 11‰. It is highly unlikely that biological remineralization could cause any of the changes observed at Station M. The 25 m casts ($n = 11$) showed a range of 33‰, and all data points except one fit a simple wind-driven model of the upper ocean. From this, we postulate that wind-driven mixing is an important

influence on the surface ocean DIC $\Delta^{14}C$. The same model failed to reproduce the variability observed at 85 m (range = 53‰, $n = 9$). In particular, wind mixing could not produce $\Delta^{14}C$ variations of the magnitude observed seasonally at Station M. We hypothesize that 85 m bottle casts sampled in and out of the California Current, sampling high DIC $\Delta^{14}C$ California Current waters during the summer when southward flow was at its maximum in strength and depth, and lower DIC $\Delta^{14}C$ waters from below the California Current in the late fall and winter when southward flow was at its minimum.

Variability in DIC $\Delta^{14}C$ was highest at 450 m (a range of 53‰, $n = 7$). 450 m DIC $\Delta^{14}C$ did not covary with 25 or 85 m DIC $\Delta^{14}C$, but it did covary with 700 and 1600 m DIC. The covariation of intermediate depth DIC $\Delta^{14}C$ values is consistent with quasi-seasonal depressions in the density field caused by the Point Conception Eddy. The northward-flowing California Undercurrent varies in strength and location, but there are not enough available physical oceanographic data to understand the effects of California Undercurrent changes on the $\Delta^{14}C$ of DIC at intermediate depths.

The least variability occurred at 1600 and 2500 m. Notably, the variability at 2500 m was within our experimental error. Our average value at this depth was within 3‰ of the WOCE value for this depth taken at a site very close to Station M.

At 3500 and 4050 m the variability increased, with 3500 m showing a range of 32‰ ($n = 5$) and 4050 m showing a range of 23‰ ($n = 6$). It is unlikely that this variability is caused by organic matter remineralization. It remains unclear what physical processes could cause variability in the DIC $\Delta^{14}C$ at depth.

Acknowledgements

We are grateful to Michaele Kashgarian, John Southon, and their coworkers at LLNL for their AMS analysis of the samples reported here. We thank Sheila Griffin, Dave Wolgast, Beth Gaza, Mark Schrope, and Ai Ning Luo for collection of samples at sea. We acknowledge Ann McNichol and colleagues at Woods Hole Oceanographic Institution for the preparation of Pulses 7 and 11 DIC samples. We appreciate the work of Mousamy Rashid in preparing Pulse 29 and 30 samples. We thank Ken Smith and his colleagues at SIO for shared ship time. We are grateful to Sue Trumbore and Shuhui Zheng for the use of their graphite line and for their counsel. We benefited from the kind advice of J.L. Reid, A.W. Mantyla, and T.L. Hayward. Thanks go to C. Eben Franks for processing the $\delta^{13}C$ samples reported here, and we thank the crews of the R/V Atlantis II and the R/V New Horizon for their help at sea. We also thank Pete Williams for guidance in experimental design. E.R.M. Druffel and C.A. Masiello were funded by NSF grants OCE-9417391; C.A. Masiello also acknowledges NSF grant DGE-9454066. J.E. Bauer acknowledges the support of NSF grants OCE-9101540 and OCE-9501531.

References

Bauer, J.E., Druffel, E.R.M., Williams, P.M., Wolgast, D.M., Griffin, S., 1996. Inter- and intra-annual variability in isotopic (^{14}C and ^{13}C) signatures of dissolved organic carbon in the Eastern North Pacific. Journal of Geophysical Research 101 (C9), 20 543–20 552.

Bauer, J.E., Druffel, E.R.M., Wogast, D.M., Griffin, S., Masiello, C.A., 1998. Distributions of dissolved organic and inorganic carbon and radiocarbon in the eastern North Pacific continental margin. Deep Sea Research II 45, 689–713.

Beaulieu, S., Baldwin, R., 1998. Temporal variability in currents and the benthic boundary layer at an abyssal station off central California. Deep Sea Research II 45, 587–615.

Broecker, W.S., Mix, A., Andree, M., Oeschger, H., 1984. Radiocarbon measurements on coexisting benthic and planktonic foraminifera shells; potential for reconstructing ocean ventilation times over the past 20,000 years. Nuclear Instruments and Methods in Physics Research B 4, 331–339.

Broecker, W.S., Peng, T.-H., 1980. Seasonal variability in the $^{14}C/^{12}C$ ratio for surface ocean water. Geophysical Research Letters 7 (11), 1020–1022.

Broecker, W.S., Peng, T.-H., 1982. Tracers in the Sea. LDGO Press.

Brown, T.A., Farwell, G.W., Grootes, P.M., Schmidt, F.H., Stuiver, M., 1993. Intra-annual variability of the radiocarbon content of corals from the Galapagos Islands. Radiocarbon 35, 245–251.

Druffel, E.R.M., 1987. Bomb radiocarbon in the Pacific: annual and seasonal timescale variations. Journal of Marine Research 45, 667–698.

Druffel, E.R.M., 1989. Decade time scale variability of ventilation in the North Atlantic: high-precision measurements of bomb radiocarbon in banded corals. Journal of Geophysical Research 94, 3271–3285.

Druffel, E.R.M., Griffin, S., Bauer, J.E., Wolgast, D.M., Wang, X.C., 1998. Distribution of particulate organic carbon and radiocarbon in the water column from the upper slope to the abyssal northeast Pacific Ocean. Deep Sea Research II 45, 667–687.

Druffel, E.R.M., Bauer, J.E., Williams, P.M., Griffin, S., Wogast, D., 1996. Seasonal variability of particulate organic radiocarbon in the northeast Pacific Ocean. Journal of Geophysical Research 101 (C9), 20 543–20 552.

Druffel, E.R.M., Williams, P.M., Bauer, J.E., Ertel, J., 1992. Cycling of dissolved and particulate organic matter in the open ocean. Journal of Geophysical Research 97, 15 639–15 659.

Duffy, P.B., Caldeira, K., 1995. Three-dimensional model calculation of ocean uptake of bomb ^{14}C and implications for the global budget of bomb ^{14}C. Global Biogeochemical Cycles 9, 373–375.

Fiadero, M., 1982. Three-dimensional modeling of tracers in the deep Pacific Ocean II. radiocarbon and the circulation. Journal of Marine Research 40, 537–550.

Freeland, H.J., 1993. Intense currents in the deep northeast Pacific Ocean. Journal of Physical Oceanography 23, 1872–1876.

Hayward, T.L., 1993. Preliminary observations of the 1991–1992 El Niño in the California Current. California Cooperative Oceanic Fisheries Investigations Reports 34, 21–29.

Hayward, T.L., Mantyla, A.W., Lynn, R.J., Smith, P.E., Chereskin, T.K., 1994. The state of the California Current in 1993–1994. California Cooperative Oceanic Fisheries Investigations Reports 35, 19–35.

Hickey, B.M., 1979. The California Current System – hypotheses and facts. Progress in Oceanography 8, 191–279.

Jones, B.H., Mooers, C.N.K., Rienecker, M.M., Stanton, T., Washburn, L., 1991. Chemical and biological structure and transport of a cool filament associated with a jet-eddy system off Northern California in July 1986 (OPTOMA 21). Journal of Geophysical Research 96 (C12), 22 207–22 225.

Key, R.M., Quay, P.D., Jones, G.A., McNichol, A.P., vonReden, K.F., 1996. WOCE AMS radiocarbon I: Pacific Ocean results (P6, P16 and P17). Radiocarbon 38 (3), 425–518.

Koblinsky, C.J., Simpson, J.J., Dickey, T.D., 1984. An offshore eddy in the California Current System part II: surface manifestation. Journal of Physical Oceanography 13, 51–69.

Levin, I., Graul, R., Trivett, N.B., 1995. Long-term observations of atmospheric CO_2 and carbon isotopes at continental sites in Germany. Tellus 47B, 23–34.

Lukas, R., Santiago-Mandujano, F., 1996. Interannual variability of Pacific deep- and bottom-waters observed in the Hawaii Ocean Time-series. Deep Sea Research II 43, 243–255.

Lynn, R.J., Schwing, F.B., Hayward, T.L., 1995. The effect of the 1991–1993 ENSO on the California Current System. California Cooperative Oceanic Fisheries Investigations Reports 36, 57–71.

Lynn, R.J., Simpson, J.J., 1987. The California Current System: the seasonal variability of its physical characterisitcs. Journal of Geophysical Research 92 (C12), 12 947–12 966.

Lynn, R.J., Simpson, J.J., 1990. The flow of the Undercurrent over the continental borderland off southern California. Journal of Geophysical Research 95 (C8), 12 995–13 008.

Mantyla, A.W., Reid, J.L., 1983. Abyssal characteristics of the world ocean waters. Deep Sea Research 30, 805–833.

McNichol, A.P., Jones, G.A., Hutton, D.L., Gagon, A.R., Key, R.M., 1994. The rapid preparation of seawater sigma-CO_2 for radiocarbon analysis at the National Ocean Sciences AMS facility. Radiocarbon 36, 237–246.

Nydal, R., Loveseth, K., Gulliksen, S., 1979. A survey of carbon-14 variations in nature since the test ban treaty. Proceedings of the Ninth International Conference on Radiocarbon Dating 9, 313–323.

Ostlund, H.G., Stuiver, M., 1980. GEOSECS Pacific radiocarbon data. Radiocarbon 22, 25–53.

Owen, R.W., 1980. Eddies of the California Current System: physical and ecological characteristics. In: D.M. Power (Ed.), California Islands: Proceedings of a Multidisciplinary Symposium, pp. 237–261. Santa Barbara Museum of Natural History.

Quay, P.D., Stuiver, M., Broecker, W.S., 1983. Upwelling rates for the equatorial Pacific Ocean derived from the bomb ^{14}C distribution. Journal of Marine Research 41, 769–792.

Robinson, S.W., 1981. Natural and man-made radiocarbon as a tracer for coastal upwelling processes. In: F.A. Richards (Ed.), Coastal Upwelling, pp. 298–302.

Rodgers, K.B., Cane, M.A., Schrag, D.P., 1997. Seasonal variability of sea surface $\Delta^{14}C$ in the equatorial Pacific in an ocean circulation model. Journal of Geophysical Research 102 (08), 18627–18639.

Sheres, D., Kenyon, K.E., 1990. An eddy, coastal jets and incoming swell all interacting near Pt. Conception, California. Journal of Remote Sensing 11 (2), 5–25.

Stuiver, M., Ostlund, H.G., Key, R.M., Reimer, P.J., 1996. Large-volume WOCE radiocarbon sampling in the Pacific Ocean. Radiocarbon 38 (3), 519–562.

Stuiver, M., Polach, H.A., 1977. Reporting of ^{14}C data. Radiocarbon 19 (3), 355–363.

Sverdrup, H.U., Fleming, R.H., 1941. The waters off the coast of southern California, March to July 1937. Bulletin of the Scripps Institute of Oceanography 4, 261–378.

Toggweiler, J.R., Dixon, K., Bryan, K., 1989. Simulations of radiocarbon in a coarse-resolution world ocean model 1. Steady state prebomb distributions. Journal of Geophysical Research 94 (C6), 8217–8242.

Vogel, J.S., 1992. Rapid production of graphite without contamination for biomedical AMS. Radiocarbon 34, 344–350.

Williams, P.M., Druffel, E.R.M., 1987. Radiocarbon in dissolved organic matter in the central north Pacific ocean. Nature 330, 246–248.

Williams, P.M., Linick, T., 1975. Cycling organic carbon in the ocean: use of naturally occuring radiocarbon as a long and short-term tracer. I.A.E.A. Report SM-191-26, 153–165.

Woodruff, S.D., Lubker, S.J., 1993. Comprehensive ocean-atmosphere data set (COADS) release 1a: 1980–1992. Earth System Monitor 4, 1–8.